# An Investigation of the Feasibility of Employing Hydroacoustic Monitoring as a Means to Detect the Presence and Movement of Large, Adult Eels (Genus *Anguilla*)

Alex Haro[1], Don Degan[2], John Horne[3], Brandon Kulik[4], And Jacques Boubee[5]

CAFRC Internal Report No. 99-01

January, 1999
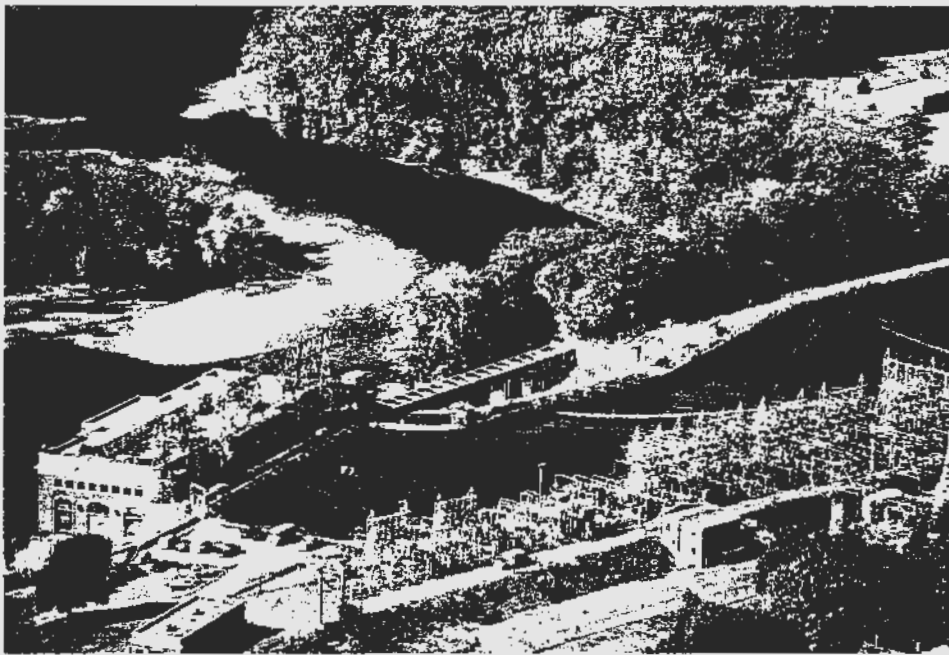
Cabot Station forebay, Connecticut River, Turners Falls, MA

[1]S. O. Conte Anadromous Fish Research Center, U.S. Geological Survey Biological Resources Division, Turners Falls, MA 01376

[2]Aquacoustics, Inc. 816C Brawley School Rd., Mooresville NC 28117

[3]Great Lakes Environmental Research Laboratory/NOAA, 2205 Commonwealth Blvd., Ann Arbor, MI 48105

[4]Kleinschmidt Associates, 75 Main St., Pittsfield, ME 04967

[5]National Institute for Water and Atmospheric Research, Gate 10, Silverdale Rd., Box 11-115, Hamilton, New Zealand

An Investigation of the Feasibility of Employing Hydroacoustic Monitoring as a Means to Detect the Presence and Movement of Large, Adult Eels (Genus *Anguilla)*

I   INTRODUCTION

The management and conservation of world wide eel populations has become an issue of heightened concern in recent years, especially in North America, Europe, Asia and New Zealand. In the U.S., concerns have been raised regarding a significant increase in commercial harvest throughout most of the species' North American range, and a growing perception that recruitment to the fishery is declining at least in some river basins. Although the extent of, and causes for, this apparent decline are not documented, in recent years there has thus been growing concern among resource management agencies that greater measures must be taken to conserve remaining eel resources (ASMFC, in prep.). Fishery managers have expressed concern over potential human impacts, including mortality due to commercial over-exploitation, pollution, habitat destruction, and upstream and downstream passage at dams.

As a consequence, resource agencies have in some instances requested downstream passage improvements for adult emigrant eels at dams. However, most conventional fish passage designs are historically based on the biological and behavioral requirements of anadromous salmonids and clupeids. Recent observations indicate that eel migration patterns differ from those exhibited by anadromous fishes, and eel movements may vary site-specifically; thus conventional passage designs employed for other species may not effectively attract and pass eels. Little detailed behavioral information exists regarding eel movements during migration.

Examples of information important to the downstream eel passage issue are: Are eel outmigration movements primarily nocturnal or diurnal? Will eels respond predictably to light, sound, hydraulic or other stimuli? Where in the water column do eels swim when migrating? Do they "search" for a particular downstream outlet or attempt to pass whatever intake location they happen to encounter? What attracts or repels eels in a forebay? Do eels school or move individually? Will they pass via spillways and gates?

Study methods to reveal the timing, behavior, spatial and temporal patterns of eel movements during emigration have thus far been limited to transmitter tagging and anecdotal observation. Thus conclusive information regarding eel movement at dams is limited. Haro and Castro-Santos (1997) investigated adult American eel (*Anguilla rostrata*) movements in a Connecticut River canal, using acoustic and radio telemetry. Barbin et al. (1998) also employed acoustic tags to investigate silver-phase American eel movements in the Penobscot River, Maine. However, telemetry methods have limitations, such as:

> (a) small sample size
> (b) potential for alteration of the behavior of test specimens
> (c) limited resolution of spatial data
> (d) potentially high labor and material costs if the study objective is to track a

significant number of eels and/or monitor movement for an extended time period

(e) loss of signals in deep water intakes and/or acoustic or electrical interference

(f) tag transmitter or retention failure potentially confounding results

(g) difficulty in discerning individual or school responses

An alternate method for observing the movement, spatial and temporal patterns of fish is hydroacoustic surveillance. This method has been successfully used to both enumerate and evaluate movements of migratory salmonids and clupeids. In general, hydroacoustics works best when:

(a) the fish target of interest has a predictable and unique echo pattern, due either to uniform size, morphometry, or known general timing and abundance in the study area

(b) the acoustic environment is relatively free of interference from turbulence, acoustic/electrical interference and false echoes

Although it has never been applied to the aquatic movements of eels, hydroacoustics has the potential to define critical aspects of eel behavior relative to fish passage if it can acceptably detect eel targets under a suitable range of conditions. Brandt (unpublished data) experimentally used hydroacoustics to survey for eels in an open ocean environment. However, the feasibility of hydroacoustic sampling for eels in freshwater has not been explored, although it potentially represents an effective way to evaluate riverine movement and responses at instream barriers and stimuli.

Hydroacoustics has several inherently advantageous characteristics:

(a) it can record the spatial patterns of individual or large numbers of targets over time without intrusive transmitters or risk of altering the behavior of the test subject

(b) a large area of river and/or any depth of intake or canal, etc. can be monitored

(c) real-time movements can be field-observed and recorded

(d) fixed aspect monitoring can be automated to operate indefinitely, minimizing labor costs associated with long-term data gathering

Hydroacoustics also has potential limitations:

(a) target discrimination is based on interpretation of fish echo patterns, which in turn can be influenced by localized environmental or physical site factors

(b) spatial sampling may require making and testing assumptions, or additional validation with supplementary field techniques

(c) it may be difficult to satisfactorily ensonify the entire passage zone of interest – i.e., fish located along walls, stream bottoms, or in zones of turbulence may not be detectable.

II OBJECTIVES

The primary objective of this pilot study is to evaluate whether adult eel echoes (corresponding in size to those migrating downstream) can be adequately discriminated from other common fish acoustic targets under both laboratory and field conditions. The focus of the application is limited to evaluating parameters necessary only for the purpose of gathering information on the spatial and temporal movement, and swimming behavior of eels in a riverine environment. Evaluation of methods to develop a quantitative estimate of the number of eels passing a point of interest, another potentially valid use of acoustic sampling, is beyond the scope of this investigation.

We have chosen to characterize acoustic signatures from American eels and develop a mathematical acoustic model for this and two additional species of freshwater australasian eels; the shortfinned (*A. australis*) and longfinned (*A. dieffenbachii*) eel. The latter two species are under similar impact from hydroelectric development and loss of habitat, and the acoustic estimates will be useful for future hydroacoustic surveys in New Zealand and Australia.

In this report we will:

   (a) identify target strength and signature characteristics of adult eel under various orientations to the transducer
   (b) evaluate an application of using a fixed-aspect hydroacoustic system to detect in-field eel movements
   (c) provide guidelines and recommendations specifically for applied use of hydroacoustic monitoring for evaluation of behavior and timing of eel movement

III METHODS

Study Sites
Estimates of eel target strength were performed at the S. O. Conte Anadromous Fish Research Center (CAFRC), Turners Falls, Massachusetts. Live adult American eels were obtained from the Millers River (tributary of the Connecticut River, Franklin County, Massachusetts) and Cobbosee Stream (tributary of the Kennebec River, Kennebec County, Maine) in July and August, 1998. Eels were held unfed in concrete flow-through holding ponds (Burrows and Chenoweth 1970) at the CAFRC facility and supplied with ambient Connecticut River water (21 - 24 °C). Hydroacoustic calibration and target strength tests were performed in an isolated section of a second holding pond (Fig. 1) measuring 10 m x 1.75 m x 2 m water depth on August 27 and 28 (water temperature 24 °C). Monitoring of downstream migrant eel passage was performed in the forebay of Cabot Station, a 51 megawatt hydroelectric facility 0.5 km downstream of the Conte Laboratory on the Connecticut River (Fig. 2).

Eel Target Strength Determination
We used a Biosonics DT6000 digital echosounder (DT Acquisition v3.05 software) with a 420kHz split beam transducer (6° x 12° beam width) mounted at one end of the holding pond 1 m from the bottom. A standard spherical calibration target with known echo image characterisitcs was suspended on the axis of the acoustic beam. The acoustic

3

environment was placid and clean (i.e.. water not flowing, and debris-free). It was necessary to subdue test specimens so that the fish would remain in the beam long enough for the desired number of pings to be collected. We sampled with both 0.4 and 0.5 msec pulse widths at a sample rate of 5 pings/second. Eels were anesthetized in MS-222 or killed immediately before testing and suspended vertically in the water at mid depth (approximate center of transducer beam) from a bracket located above the pond by an attached single monofilament nylon line at a horizontal distance of 7 m from the transducer. Target strengths (dorsal and lateral aspects) were measured for six test eels of varying sizes (350, 355, 580, 610, 670, and 685 mm SL). Test eels were then transported on ice to an x-ray facility and radiographs were taken of dorsal and lateral aspects of each fish.

Cabot Station Forebay Monitoring
To qualitatively verify the relative abundance of eels in the forebay during the hydroacoustic surveillance period. an underwater closed-circuit video camera was installed in the bypass weir to record passage of eels and other fishes. The bypass weir is located at the southern end of the station intake, and was outside the ensonified zone of the forebay (Fig. 2). The bypass weir was illuminated by a 1000 watt mercury vapor and 1000 watt sodium vapor lamp that are used for attraction of juvenile anadromous clupeids to the bypass. A sampling device that intercepts all fish passing the bypass is located downstream of the bypass weir. To enhance image contrast, a 1 m wide band extending across the floor of the bypass weir and the wall opposite the camera was painted white. Video recording was performed using time lapse video recorders (12 h mode; approximately 4 frames/sec) capable of logging the date and time of each passage event. Video recording was begun on 9 September and ended 14 November, but only during the night hours (17:00 to 05:00). Temperature data from the Cabot Station canal were logged on an hourly basis for the duration of the study. Flow data from the Connecticut River mainstem were obtained from the USGS gauging station at Montague City (2 km downstream of Cabot Station). Additional flow data were collected from the USGS gauging station on the Millers River, a tributary of the Connecticut River, at Erving (10 km upstream from Cabot Station). The Millers River is not subject to alteration of flow by hydropower facilities. Daily rainfall data from a NOAA weather station in Sunderland, MA (approximately 20 km from Cabot Station) were obtained from the NOAA Climatic Data Center.

A field test to detect potential acoustic eel targets was performed in the forebay of Cabot Station. The objective of this test was to determine if it was feasible to qualitatively gather information on the timing and magnitude of eel movement in a section of the forebay with the type of acoustic equipment and target strength information gathered in the test pond. The test was performed using the same echosounder, 420 kHz split beam transducer, and software that was used in target strength estimation tests. The transducer was mounted from a steel pole next to a concrete forebay wall 6.5 m upstream of the trash racks at a depth of 1 m, with the beam oriented across the forebay at an angle 12° upstream from a line parallel to the racks (Fig. 2), and downward at an angle of 5°. This configuration allowed us to sample at maximum range (40 m) across the forebay in an area just upstream of the trash racks, where eels have been observed at the surface swimming against the flow. The far end of the beam cone also sampled from the surface to the bottom (10 m). Precise beam position was determined

by suspending a lead target at known three-dimensional positions relative to the transducer, recording target strengths for a two minute period, and calculating beam position based on a matrix of target position and strengths.

Hydroacoustic monitoring for eel targets in the forebay began on 17 September and terminated on 5 October. The DT system sampled at 5 pings/second with a threshold of −50 dB and pulse width of 0.4 msec. Because of the large quantities of data collected, the threshold was increased to −41 dB during the overnight period of 23 - 24 September. The threshold was reduced back to -50 dB on 24 September, since larger targets appeared to be missed at the higher threshold setting. Monitoring was performed at night only, from sundown to sunrise (from approximately 18:30 to 06:30) daily. Hydroacoustic data were downloaded from the control computer on a daily basis, stored to disk, verified, and sent to Aquacoustics, Inc. for processing and analysis.

Acoustic Model
Dorsal and lateral radiographs of five American eels that were used in the target strength determination tests were converted to digital silhouettes by tracing the outer edges of bodies (not including fins) and swimbladders. Additional radiographs and tracings of one longfinned and two shortfinned eels were provided by J. Boubée, National Institute for Water and Atmospheric Research (NIWA), Hamilton, New Zealand. Tracings were then scanned and digitized at 1 mm resolution along the medial axis of the fish body using an automated algorithm. Dorsal and lateral body outlines traced on velum were used to check accuracy of body edge delineation on radiograph tracings.

IV DATA ANALYSIS

Eel Target Strength Determination
We analyzed the eel target strength by processing the data files through BioSonics DT Analyzer Version 3.1.1 software and outputting a database with echo location, target strength, and range. This database was filtered to remove targets other than from the eel as well as targets greater than 2 dB off axis. The remaining targets are averaged to provide mean target strength for each eel sampled. These data are then regressed with the Log_{10} (total length) of the eel.

Cabot Station Forebay Monitoring
Videotapes from the Cabot Station bypass camera for the period from 18 September to 4 October were reviewed in their entirety (17:00 to 05:00) at approximately 5X normal speed. Fish passing the weir were identified to species (when possible) and recorded along with time of passage. A second reviewer assisted in identifying objects or fish that could not be characterized by the first reviewer. Counts of eels were summed on a daily and hourly basis; hourly counts were analyzed to determine patterns of frequency in eel passage over the nocturnal observation period. Because river flows increased significantly after 9 October, we also reviewed videotapes for the early evening hours (17:00 to 22:00) for the period from 5 October to 22 October in order to compare eel counts at the bypass during this freshet.

We analyzed the Cabot Station forebay acoustic data through BioSonics DT Vtracker

Version 0.98 software and output a database with tracked fish target strength, range, number of pings for each fish, and direction of travel through the beam. Because most downstream migrant eels captured at the Cabot bypass sampler are greater than 70 cm TL. we filtered these tracked fish by selecting only those exceeding a mean target strength of -32.3 dB (70 cm) and –28.8 dB (100 cm). Counts of tracked fish were summed on a daily and hourly basis; daily and hourly counts were analyzed to determine patterns of frequency in eel passage over the period sampled and the nocturnal observation period. We noted that counts of eels during the evening of 23 September and morning of 24 September were roughly an order of magnitude greater than on other nights. Because threshold settings for the echosounder were altered during this period, the numbers of fish for this time period are probably artificially inflated (Tables 4 and 5). We therefore omitted data from this time period from all subsequent analyses.

Acoustic Model
A Kirchhoff-ray mode (KRM) model (Clay and Horne 1994) was used to estimate dorsal and lateral backscatter as a function of fish length, aspect, and acoustic carrier frequency for each eel. The KRM model coherently sums backscatter from a set of fluid-filled cylinders representing the body and a set of gas-filled cylinders representing the swimbladder. The model is parameterized for each eel and lengths are scaled for comparison. Full details of the model can be found in Clay and Horne (1994), Jech et al. (1995), or Horne and Jech (1999). Model backscatter values have been shown to match field measurements (Clay and Horne 1994; Jech et al. 1995) and the model has been applied to other species at numerous frequencies (Jech et al. 1995; Horne and Jech 1999). To quantify variation in backscatter amplitudes among American eels, the mean and standard deviation backscatter was predicted for dorsal and lateral orientation as a function of eel length, aspect, and acoustic wavelength. The fit of the model to measured target strengths was compared by plotting mean dorsal and lateral backscatter curves at 420 kHz and superimposing mean dorsal and lateral target strength values from five eels measured at the CAFRC holding pond. Trends in American eel backscatter response curves were compared to backscatter response curves of longfinned and shortfinned eels.

V RESULTS

Eel Target Strength Determination
Observed target strengths from backscatter measurements of individual eels in the holding pond varied by as much as 20 dB within sets of dorsal or lateral measurements. There were no consistent trends in amplitudes of dorsal (Fig. 3a) or lateral (Fig. 3b) backscattered echoes over time for each fish. Target strength measures also varied as a function of angle off the acoustic axis. Changes in angle off axis are due to lateral movement by the fish relative to the transducer face. To limit the amount of lateral movement included in the target strength data sets, only target strength measurements located within 3 degrees of the acoustic axis (i.e. the half power points of the transducer beam pattern) were included in comparison with predicted echo amplitudes. At a distance of 6.5 meters, this includes all targets within a 1.37 m swath along the wide axis (i.e. x-y plane) of the acoustic cone. Backscattered echo amplitudes also varied as a

function of range from the transducer (Fig. 4a, b). Changes in distance from transducer also results because of movements or swaying by the animal. To limit the amount of range variability in acoustic measurements, observed target strength data sets were also filtered to include all targets at the modal range and those within 2 cm of the modal distance (Table 1). The combination of these two filters reduced the number of targets included in average target strength and variance calculations within data sets.

The mean target strength for both dorsal and lateral aspect along with combined dorsal and lateral aspect for each of the 8 eels sampled is regressed with the total length (cm) for each eel. The three regression equations generated are:

$$TS = 19.80 \ LOG(L) - 68.95 \text{ for dorsal aspect}$$

$$TS = 19.78 \ LOG(L) - 69.12 \text{ for lateral aspect}$$

$$TS = 22.42 \ LOG(L) - 73.59 \text{ for a combined aspect.}$$

These equations were used to generate a predicted acoustic target size for eels expected in the Cabot Station forebay during sampling in September and October 1998. Differences among the predicted length for the three equations was 3 cm at –32 dB to 10 cm at –29 dB for the lengths of eels found in the bypass during the sample period. Love's (1977) any aspect equation

$$TS = 20 \ LOG(L) - 69.23$$

predicts similar lengths to the eel equations derived from our tests (Table 2). Since we could not determine which aspect the acoustic system was sampling the eels in the forebay area, we used the combined equation to predict lengths for data analysis.

Cabot Station Forebay Monitoring
Field conditions (temperature, flow, and rainfall) for the months of September and October are given in Figs. 5a and b. Water temperatures were above normal and flows were below normal for the survey period. Drifting debris was relatively minimal throughout the survey period, and consisted largely of clumps of aquatic macrophytes (primarily *Vallisneria.* sp.) 0.25 to 0.5 m in diameter.

During video monitoring, night illumination of the bypass weir and water clarity were always sufficient to view completely across the 2.5 m weir, although not all fish-like objects could be identified to species (25.7 % of total number of identifiable and unidentifiable fish). Numbers of eels passing the weir on a nightly basis were relatively low (< 1 eel/h) during the period of hydroacoustic sampling (Tables 3 and 4, Fig. 6). A small increase in the number of eels at the bypass was noted on 1 October. However, counts of eels at the bypass weir on 8 October were an order of magnitude higher than on previous nights when hydroacoustic sampling was ongoing. Overall movement of eels through the bypass tended to occur in the early evening hours (Fig. 7).

Filtering the hydroacoustic data by size range produced varying results. The temporal distribution of tracked fish greater than 70 cm in the Cabot Station forebay indicated a

peak in activity on the morning of September 23 and evening of September 24 (Table 3, Fig. 6a). A peak in numbers of targets greater than 100 cm occurred on September 23 and 24 (Table 4, Fig. 6a). The highest target detection rate occurred between 18:00 and 20:00 hours (Fig. 7a). Plotting the range and depth distribution for fish greater than 100 cm showed no trends for range across forebay or depth strata (Fig. 8). Fish greater than 100 cm did show a propensity for clumping as we observed 5 fish within a 7-minute period after sunset on September 23 (Fig. 9). Sample size for acoustics was 894 tracked fish greater than 70 cm and 84 greater than 100 cm (these only comprised 2% of the total fish tracked during the period).

Length distribution data from bypass sampler collections made in 1996 and 1997 was similar to that estimated from acoustically tracked fish (Fig. 10). Daily run timing for eels in the bypass was somewhat similar to acoustically tracked fish greater than 70 cm, but more closely resembled distribution for fish greater than 100 cm (Fig. 6a,b). Diel movements of acoustically tracked eels and eels observed in the bypass also showed some similarity (Fig. 7a,b), but the relationships between both daily and diel acoustic and video counts were low ($r^2 < 0.1$) and not statistically significant ($p < 0.05$).

Acoustic Model
Lengths of the five modeled American eels ranged from 362 mm to 691 mm with a mean length of 540 mm. The swimbladder of each fish is located below the spinal column in the anterior half of the body (Fig. 11). All swimbladders used in modeling exercises remained inflated in the radiographs. Anterior pneumatic ducts and swimbladders contained variable amounts of air.

The general shape of backscatter response surfaces was similar among and between dorsal (Fig. 12) and lateral (Fig. 13) orientations for all American eels. All fish were modeled at a length of 540 mm, through an aspect range of 70° to 110°, and an acoustic frequency range of 12 kHz to 420 kHz. Backscatter amplitudes were uniformly low at large deviations from horizontal (i.e., orthogonal to the incident acoustic wave front), and increased to a maximum near 90° (Table 5). This represents a fish orthogonal to a transducer face with no difference in the angle of swimbladder relative to the fish body. Along the fish length to acoustic wavelength axis, if fish length L is kept constant, a higher L/λ value corresponds to a higher acoustic carrier frequency. Keeping the frequency constant illustrates the effect of changes in fish length on echo amplitude. Overall, there is less influence of fish aspect on target strength at low L/λ values. Throughout the L/λ range, the response surface is symmetric about the peak echo amplitude in dorsal and lateral backscatter response curves. The quasi-periodic peaks and valleys along the 90° aspect angle correspond to areas of constructive and destructive backscatter interference. Peak dorsal backscatter amplitudes exceed maximum lateral amplitudes for all eels.

Similarities and differences among laterally and dorsally oriented backscatter curves are clarified in the mean and standard deviation backscatter response surfaces. Amplitudes and variability in the dorsal orientation average surfaces (Fig. 14a) exceed those in the average lateral orientation plots (Fig. 14b). The decreased dependence of backscatter amplitude on aspect at low L/λ values is present in both surfaces. Peak amplitudes at

any L/λ value occur at approximately 90° and decrease symmetrically as aspect angle deviates from horizontal. Standard deviation values are highest along aspect angles approximating 90°. A second area of high variability occurs in both orientations at aspects of 80° and L/λ values greater than 50. Variability in backscatter amplitudes is low at both orientations at aspects that deviate greater than 5° from horizontal.

The fit of the Kirchhoff-ray mode backscatter models to measured target strengths was examined by plotting predicted and observed mean target strength values at 420 kHz as a function of eel length over a range of 350 mm to 700 mm for dorsal and lateral orientations (Fig. 15). Dorsal and lateral predicted backscatter amplitudes non-monotonically increase as fish length increased. Predicted target strengths ranged from approximately -30 dB at 700 mm to -42 dB at 350 mm. At lengths greater than 400 mm, predicted dorsal backscatter amplitudes always exceeded predicted lateral backscatter amplitudes. With the exception of the second smallest eel (355 mm), observed mean lateral backscatter amplitudes always exceeded observed mean dorsal target strengths. Observed dorsal mean target strengths were biased low relative to the KRM model while observed lateral mean target strengths were biased high relative to the predicted backscatter.

American eel predicted backscatter response curves differed from the New Zealand longfinned and shortfinned eel backscatter response curves. The New Zealand longfinned eel dorsal response surface (Fig. 16), modeled at a fish length of 1260 mm, is distinctly different from the American eel response surfaces. The longfinned eel response surface contains a strong peak amplitude of 0.283 (-8.9 dB) at 92° aspect and a L/λ value of 252 (292 kHz). Backscatter amplitudes remain high at larger L/λ values but are relatively low at other aspect and L/λ combinations. Reduced scattering length values drop rapidly when aspect deviates from horizontal. The shortfinned eel dorsal response surface (Fig. 17) contains features similar to those observed in the American eel response surface. Backscatter from the shortfinned eel swimbladder was modeled as three separate chambers that included the anterior pneumatic duct. Backscatter amplitude was not as dependent on aspect at low L/λ values as it was at higher L/λ values. Predicted reduced scattering length peaked (0.128, -20.18 dB) at 376 kHz and 89° aspect. Maximum backscatter amplitudes generally increased with increasing L/λ values and decreased as aspect angles deviated from horizontal.

VI DISCUSSION

Eel Target Strength Determination
Target strengths as determined from testing in the holding ponds yielded predictive equations that were similar to Love's (1977) any-aspect equations for a generalized fish. This result makes it impossible to discriminate eels from other similarly-sized (TL) fishes based on target strength alone. However, the abundance of species present in the Cabot canal other than eels that are larger then 70 cm TL (e.g., adult common carp (*Cyprinus carpio*), northern pike *(Esox lucius)*, large adult smallmouth bass (*Micropterus dolomieu*), and walleye (*Stizostedion vitreum*); A. Haro, pers. obs.) is low, and few if any fish of this size were observed in the bypass. Variability in measured TS between eels within the 50 – 100 cm size range could probably be reduced by additional estimates of TS from a

9

larger sample size. A test environment with less acoustic reverberation than the Burrows ponds would also reduce variability of TS estimates.

Cabot Station Forebay Monitoring

Given the results of the target strength estimates, there was no method to unequivocally determine whether "eel-sized" targets were in fact migrant eels, since TS of other species known to be present in the Cabot forebay are comparable to those measured for smaller eels. However, some indirect evidence supports the possibility that most of the eel-sized targets were in fact eels: 1) eels comprised the greatest proportion of large fish species observed at the bypass weir, and; 2) vertical and horizontal distribution of eel-sized targets within the forebay was uniform, which reflects behavior of radio-tagged eels in the forebay observed in previous telemetry studies (Haro and Castro-Santos 1997). From nighttime visual observations at Cabot Station, smallmouth bass tend to be surface- or bottom-oriented; distribution of walleye and other species is unknown. There is also the possibility that large targets could have been debris (e.g., clumps of aquatic macrophytes), but we noted that most drifting debris occurred in the upper meter of the water column, while eel-sized targets occurred at all depths.

On a nightly basis, the number of acoustic targets per unit time did not match counts at the bypass weir. Low numbers of eels passing the bypass weir (only several per night) may have contributed to this lack of correlation. Environmental conditions that promote downstream migration in eels (Vøllestad et al. 1986) were not favorable during the two week monitoring period, as river flow and water temperature decrease were minimal. Also, we did not observe the high numbers (>10 per night) of eels passing the bypass weir that we recorded during high flow/rainfall dates after 8 October, or in previous years' monitoring of the bypass sampler. Relationships between the diel (hourly) video and acoustic counts are better, and the general trend (highest numbers of eels and targets in the early evening) also reflects catch patterns at the bypass sampler in previous years.

Also, canal flows were not constant during the two week hydroacoustic monitoring period, as Cabot Station generation typically varies throughout the day during low-flow period. Higher canal flows may have inherently been associated with higher target counts per unit time. The lack of accurate forebay flow data (both magnitude and flow field characteristics) prevented us from analyzing the count data with respect to flow. Also, fish in the forebay may have been counted more than once by repeatedly passing through the acoustic beam over time, while greater than 95% of all eels counted in the bypass weir were swept into the bypass channel and did not return to the forebay, and hence were counted only once. Because of these additional complicating factors, strong relationships between acoustic and bypass counts may not be expected, but a gross trend might have been evident had a larger peak in downstream movement (such as occurred on 8 October) occurred during the survey. It should also be noted that estimation of accurate counts or density of eels in the Cabot forebay were not objectives of the study, and are beyond the scope of this effort. Howerver, it appears from our results that the presence or absence of eels in the forebay and their spatial distribution can be inferred by hydroacoustic methods.

Acoustic Model

Predicted mean backscatter amplitudes differed from those measured in the CAFRC Burrows ponds. The American eels used in target strength experiments were large targets relative to the operating frequency of the echosounder. L/λ values used in the predicted and observed target strength comparison ranged from 98 to 192. Large length to wavelength ratio values indicate that echo returns from a single animal may be recorded as multiple targets and could potentially contribute to the variability observed in measured target strengths. Variability in maximum backscatter amplitudes in individual and mean predicted backscatter response curves also suggests that no specific frequency will maximize echo returns from all eels. The effect of fish aspect on echo amplitudes from dorsally or laterally oriented animals is consistent at all fish lengths and acoustic frequencies. An additional explanation for the mismatch in observed and predicted target strengths is the use of a shallow concrete pond to measure dorsal and lateral backscatter. Reverberation within the pond and the short range from transducer to target potentially contributed to the over 20 dB in target strength range observed in each set of target strength measurements.

A third procedural step that potentially contributed to the mismatch in target strengths is the time delay between target strength measurements and x-rays. Several hours elapsed between time of measurement at ambient water temperature, to storage in an ice-packed cooler, to x-ray at room temperature. The swimbladders of American eels are physostomous with a large duct joining the swimbladder and the oesophagus. The duct appears as a separate chamber and serves as a primitive lung (Steen 1963). It is not known if live eels change the volume of gas in the swimbladder and pneumatic duct while exposed to air for extended periods.

Comparison of target strengths between measured and modeled American eels ranged from 350 mm to 700 mm. This length range bracketed the range of lengths used to model eel backscatter response curves with the KRM models. Clay and Horne (1994) compared predicted target strengths of Atlantic cod (*Gadus morhua*) to maximum target strengths measured by Nakken and Olsen (1977). They found that a KRM model of a 38 cm fish matched observed scattering over a range of 8 cm to 100 cm. Since American eel swimbladder angles do not appear to vary dramatically from horizontal, modeled target strengths could be extrapolated beyond the range of lengths used in the model. High variability observed in measured target strengths and the non-monotonic increase in target strength with fish length reduces the predictive value of the KRM model.

Dorsal backscatter response curves for New Zealand shortfinned and longfinned eels were based on a single animal. The curled x-ray of the longfinned eel increased the difficulty of constructing a straight body form. The large size (1260 mm) of the longfinned eel greatly increased the predicted target strength relative to the predicted target strengths of the American eels. Higher geometric scattering frequencies result in higher predicted backscatter amplitudes. Modeling the swimbladder of the shortfinned eel as three separate chambers did not appear to influence the character of the backscatter response curve. Features in the shortfinned response curve were similar to those observed in the American eel backscatter response curves. The anterior pneumatic duct was more apparent in the shortfinned eel radiograph than in any other eel radiograph. General anatomical arrangement of swimbladder, pneumatic duct, and relative position of swimbladder in body cavity was similar among American, longfinned, and shortfinned eels.

11

VII RECOMMENDATIONS

At present, it appears that hydroacoustics can be used as a qualitative tool to determine the spatial and temporal patterns of behavior of large (> 70 cm) eels in hydroelectric forebays. Verification of targets remains a critical aspect to the usefulness of hydroacoustic data, and concurrent monitoring of actual eel abundance (e.g., by video, netting, visual observation) should be performed as part of a hydroacoustic survey protocol. Where possible, the method of verification should be carefully chosen so as to most accurately reflect abundance of targets as determined by acoustic monitoring.

Also, discrimination of eel targets from those of other fishes remains problematic, but is also site-specific. In some circumstances, downstream migrant eels may be the largest or most abundant large targets in a survey area, adding confidence to positive identification of targets as eels (in most cases, however, this will be the exception). Where possible, we recommend that TS measurements of species that may potentially confound identification of acoustic targets be made.

Other confounding factors in a hydroacoustic survey will be water turbulence and turbidity, and the presence of drifting debris. In the case of this study, these effects were minimal, but it is generally accepted that peak downstream movements of eels will occur when these conditions may at times be at their worst for acoustic monitoring (i.e., high flows).

Additional acoustic modeling should improve discrimination among eel and other acoustic targets. Comparison of American eel predicted and observed target strengths to those of other species found in the same water is the most prudent next step. If frequency-dependent target strengths differ among species then acoustic targets may be classified based on echo amplitudes or comparison of frequency-dependent echo amplitudes at more than one frequency. If target strengths are not radically different among species then quantitative measures of the echo envelope (i.e. the time-dependent amplitude of a received pulse) must be used to discriminate individual or groups of targets.

VIII ACKNOWLEDGEMENTS

also to Northeast Utilities Service Company for their cooperation, support, and use of the Cabot Station facility.

IX REFERENCES

ASMFC (Atlantic States Marine Fisheries Commission). *In prep.* Fishery management plan for the American eel *Anguilla rostrata.* Atlantic States Marine Fisheries Commission, Washington, D.C. 93 p.

Barbin, G. P., S. J. Parker, and J. D. McCleave 1998. Olfactory clues play a critical role in the estuarine migration of silver-phase American eels. Envir. Biol. Fishes 53: 283-291.

Burrows, T. E. and H. H. Chenoweth. 1970. A rectangular circulating rearing pond. Prog. Fish Cult. 32: 67-80.

Clay, C. S. and J. K. Horne. 1994. Acoustic models of fish, the Atlantic cod (*Gadus morhua*). J. Acoust. Soc. Am. 96: 1661-1668.

Steen, J. B. 1963. The physiology of the swimbladder in the eel, Anguilla vulgaris. III. The mechanism of gas secretion. Acta Physiol. Scand. 59: 221-241.

Haro, A. and T. Castro-Santos. 1997. Downstream migrant eel telemetry studies, Cabot Station, Connecticut River, 1996. S.O. Conte Anadromous Fish Research Center Internal Report No. 97-01.

Horne, J.K. and J. M. Jech. 1999. Multi-frequency estimates of fish abundance: constraints of rather high frequencies. ICES J. Mar. Sci. (in press).

Jech, J. M., Schael, D. M., and C. S. Clay. 1995. Applications of three sound scattering models to threadfin shad (*Dorosoma petenense*). J. Acoust. Soc. Am. 98: 2262-2269.

Love, R. H. 1977. Target strength of an individual fish at any aspect. J. Acoust. Soc. Am. 62: 1397-1403.

Nakken, O. and K. Olsen. 1977. Target strength measurements of fish. Rapp. P.-v. Rèun. Cons. perm. int. Explor. Mer 170: 52-69.

Vøllestad, L. A., B. Jonsson, N. A. Hvidsten, T. F. Næsje, Ø. Haraldstad, and J. Ruud-Hansen. 1986. Environmental factors regulating the seaward migration of European silver eels (*Anguilla anguilla*). Can. J. Fish. Aquat. Sci. 43: 1909-1916.

Table 1. American eel (*Anguilla rostrata*) lengths, orientations (dor = dorsal, lat = lateral), number of original target strength measurements, number of filtered target strength measurements, original mean target strength $\overline{TS}$ ± standard deviation sd, filtered $\overline{TS}$ ± sd, and corresponding KRM predicted $\overline{TS}$ ± sd based on five American eel radiographs.

Fish Length (mm)		No. Original Targets	No. Filtered Targets	Original $\overline{TS} \pm sd$	Filtered $\overline{TS} \pm sd$	Predicted $\overline{TS} \pm sd$
350	dor	562	149	-41.4 ± 3.15	-38.5 ± 1.98	-39.5 ± 4.85
	lat	672	130	-40.0 ± 3.77	-38.0 ± 1.90	-42.7 ± 5.63
355	dor	893	105	-37.1 ± 3.63	-36.0 ± 1.86	-39.1 ± 2.27
	lat	758	162	-39.4 ± 3.46	-40.2 ± 2.80	-41.6 ± 4.10
580	dor	915	682	-38.4 ± 4.39	-38.7 ± 4.18	-35.4 ± 5.63
	lat	799	260	-35.5 ± 4.59	-35.9 ± 4.01	-34.7 ± 3.19
610	dor	430	250	-36.2 ± 3.58	-34.6 ± 2.42	-33.1 ± 2.75
	lat	488	165	-32.4 ± 4.94	-29.1 ± 2.95	-40.7 ± 11.56
670	dor	908	127	-34.3 ± 4.69	-29.6 ± 1.93	-35.5 ± 12.38
	lat	773	219	-30.7 ± 4.80	-28.5 ± 2.63	-38.5 ± 8.79
685	dor	1231	444	-34.6 ± 4.73	-33.2 ± 3.57	-33.4 ± 11.59
	lat	896	200	-34.2 ± 4.53	-33.8 ± 3.74	-31.5 ± 2.61

Table 2. Predicted lengths (cm) for eels using the three target strength/length regression equations generated from data collected in the Burrows ponds in August 1998 and Love's any aspect equation.

Target size (dB)	Combined Aspect	Dorsal Aspect	Lateral Aspect	Love's Any Aspect
-36	47	46	47	46
-35	53	52	53	51
-34	58	58	60	58
-33	65	65	67	65
-32	72	73	75	73
-31	79	83	85	82
-30	88	93	95	92
-29	97	104	107	103
-28	108	117	120	115
-27	120	131	135	129
-26	133	148	151	145

Table 3. Fish activity as measured by hydroacoustics in the Cabot Station forebay September 17 through October 5, 1998. These data represent the number of fish greater than 70 cm, with the converted total lengths from an acoustic target strength relationship for eels (TS = 22.42LOG(L) - 73.59) generated at the Conte Lab prior to field sampling. Note that counts during the period from the evening of 23 September through the morning of 24 September are abnormally high (probably due to alteration of echosounder threshold settings during this period), and were omitted from the dataset in further analyses.

Hour	17-Sep	18-Sep	19-Sep	20-Sep	21-Sep	22-Sep	23-Sep	24-Sep	25-Sep	26-Sep	27-Sep	28-Sep	29-Sep	30-Sep	1-Oct	2-Oct	3-Oct	4-Oct	5-Oct	Hourly Mean Rate
0		1.0	0.0	1.0	6.0	0.0	2.0	18.0	0.0	1.0	3.0	0.0	9.0	2.0	4.0	8.0	4.0	0.0	2.0	3.4
1		0.0	1.0	0.0	0.0	2.0	7.0	15.0	1.0	4.0	1.0	3.0	12.0	1.0	1.0	8.0	1.0	5.0	2.0	3.6
2		0.0	4.0	2.0	1.0	1.0	4.0	26.0	1.0	0.0	3.0	2.0	1.0	6.0		3.0	3.0	2.0	0.0	3.5
3		0.0	1.0	0.0	1.0	1.0	3.0	42.0	4.0	2.0	5.0	0.0	2.0	3.0	2.0	4.0	3.0	2.0	0.0	4.2
4		0.0	2.0	1.0	3.0	5.0	0.0	48.0	0.0	0.0	4.0	1.0	2.0	5.0	5.0	2.0	2.0	4.0	0.0	4.7
5			1.0	3.0	0.0	7.0	0.0	58.0	0.0	0.0	2.0	1.0	0.0	2.0	3.0	3.0	2.0	3.0	1.0	5.1
6			1.0	1.0	0.0	0.0	2.0	36.0	2.0	0.0	0.0	0.0	0.0	4.0	2.0	2.0	0.0	4.0	0.0	2.9
7			0.0				4.0								0.0	0.0				1.5
8							2.0									2.0				2.0
9							2.0													2.0
10																				
11																				
12																				
13																				
14																				
15																				
16																				
17																				
18	0.0			2.0	2.0		26.0	0.0	4.0	0.0	0.0	2.7				2.7	2.7	2.7		3.6
19	0.0	1.0		3.0	9.0		45.0	6.0	0.0	5.0	0.0	13.0	1.3	4.0		15.0	5.0	4.0		7.8
20	2.0	2.0	2.0	4.0	6.0		37.0	16.0	3.0	6.0	2.0	8.0	2.0	6.0	8.0	10.0	5.0	1.0		7.2
21	4.0	0.0	0.0	3.0	5.0	3.0		15.0	0.0	7.0	5.0	9.0	2.0	8.0	4.0	3.0	2.0	2.0		4.2
22	5.0	1.0	1.0	2.0	4.0	0.0		4.0	4.0	6.0	3.0	6.0	3.0	4.0	4.0	1.0	5.0	0.0		3.1
23	1.0	0.0	1.0	4.0		3.0		5.0	0.0	2.0	0.0	4.0	3.0	5.0	4.0	3.0	1.0	2.0		2.8
Daily Mean rate	2.1	0.5	1.7	2.0	3.8	2.3	10.0	22.6	1.3	2.8	2.3	4.0	3.4	4.2	3.3	4.6	2.9	2.3	0.8	4.3

Table 4. Fish activity as measured by hydroacoustics in the Cabot Station forebay September 17 through October 5, 1998. These data represent the number of fish greater than 100 cm. with the converted total lengths from an acoustic target strength relationship for eels (TS = 22.42LOG(L) - 73.59) generated at the Conte Lab prior to field sampling. Note that counts during the period from the evening of 23 September through the morning of 24 September are abnormally high (probably due to alteration of echosounder threshold settings during this period), and were omitted from the dataset in further analyses.

Hour	17-Sep	18-Sep	19-Sep	20-Sep	21-Sep	22-Sep	23-Sep	24-Sep	25-Sep	26-Sep	27-Sep	28-Sep	29-Sep	30-Sep	1-Oct	2-Oct	3-Oct	4-Oct	5-Oct	Hourly Mean Rate
0		0.0	0.0	0.0	0.0	0.0	0.0	3.0	0.0	0.0	0.0	0.0	0.0	0.0	0.0	2.0	1.0	0.0	1.0	0.4
1		0.0	0.0	0.0	0.0	0.0	1.0	0.0	0.0	0.0	0.0	0.0	1.0	0.0	0.0	2.0	0.0	1.0	0.0	0.3
2		0.0	0.0	0.0	0.0	0.0	0.0	0.0	0.0	0.0	1.0	0.0	0.0	1.0		0.0	1.0	0.0	0.0	0.2
3		0.0	0.0	0.0	0.0	0.0	0.0	2.0	0.0	0.0	0.0	0.0	0.0	0.0	0.0	2.0	0.0	2.0	0.0	0.3
4		0.0	1.0	0.0	0.0	0.0	0.0	0.0	0.0	0.0	1.0	1.0	0.0	0.0	1.0	0.0	0.0	0.0	0.0	0.2
5			0.0	0.0	0.0	0.0	0.0	2.0	0.0	0.0	0.0	0.0	0.0	0.0	1.0	0.0	0.0	0.0	0.0	0.2
6			0.0	1.0	0.0	0.0	0.0	4.0	0.0	0.0	0.0	0.0	0.0	0.0	0.0	1.0	0.0	0.0	0.0	0.4
7				0.0			0.0								0.0	0.0				0.0
8							0.0									0.0				0.0
9							0.0													0.0
10																				
11																				
12																				
13																				
14																				
15																				
16																				
17																				
18	0.0			2.0	0.0		0.0	0.0	4.0	0.0	0.0	0.0				0.0	0.0	0.0		0.3
19	0.0	0.0		1.0	0.0		14.0	0.0	0.0	0.0	0.0	1.0	0.0	2.0		4.0	0.0	0.0		1.5
20	2.0	0.0	0.0	0.0	0.0		10.0	0.0	1.0	0.0	0.0	0.0	0.0	0.0	0.0	1.0	0.0	0.0		0.9
21	0.0	0.0	0.0	0.0	1.0	0.0		2.0	0.0	1.0	0.0	1.0	0.0	1.0	0.0	0.0	0.0	0.0		0.4
22	0.0	0.0	0.0	0.0	1.0	0.0		2.0	0.0	0.0	0.0	0.0	1.0	0.0	0.0	0.0	0.0	0.0		0.2
23	0.0	0.0	0.0	0.0		0.0		2.0	0.0	0.0	0.0	0.0	0.0	0.0	0.0	1.0	0.0	0.0		0.2
Daily Mean rate	0.3	0.0	0.2	0.2	0.3	0.0	2.1	1.3	0.2	0.1	0.2	0.2	0.2	0.3	0.2	0.9	0.2	0.3	0.2	0.4

17

Table 5. Predicted minimum and maximum reduced scattering lengths RSL and corresponding
target strengths TS, aspect angles θ (degrees), and acoustic frequencies f (kHz) of five dorsally
and laterally oriented American eels (*Anguilla rostrata*). All backscatter amplitudes were
estimated using a Kirchhoff-ray mode backscatter model (Clay and Horne 1994) and digitized
radiographs of each fish. All fish were modeled at a length L of 0.54 m. Reduced scattering
lengths can be converted to target strengths TS (dB) using: TS = 20 log(RSL) + 20 log (L).

Fish Length (mm)	Orientation	RSL_{min}	TS_{min} (dB)	$θ_{min}$ (deg)	f_{min} (kHz)	RSL_{max}	TS_{max} (dB)	$θ_{max}$ (deg)	f_{max} (kHz)
366	dorsal	0.0000554	-90.48	110	104	0.0951	-25.79	87	308
	lateral	0.0000761	-87.72	72	120	0.0758	-27.76	90	124
372	dorsal	0.000211	-78.86	75	156	0.0760	-27.73	90	28
	lateral	0.000330	-74.98	79	24	0.0654	-29.04	89	332
608	dorsal	0.0000662	-88.93	110	156	0.107	-24.76	89	68
	lateral	0.000190	-79.78	107	80	0.0763	-27.70	89	44
660	dorsal	0.0000599	-89.80	110	40	0.116	-24.06	88	344
	lateral	0.0000478	-91.76	110	128	0.0868	-26.58	90	168
691	dorsal	0.000103	-85.1	110	12	0.110	-24.52	89	148
	lateral	0.000285	-76.26	110	48	0.0793	-27.37	89	120
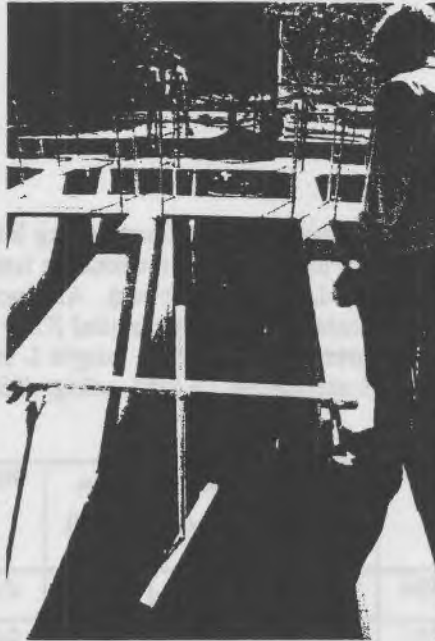
Figure 1. Acoustic measurement of eels in the Burrows pond at the Conte Laboratory. Anesthetized or freshly killed eels were suspended vertically from the rotating frame in the foreground, allowing for measurement of target strength in dorsal and lateral aspects. The transducer (not visible) was mounted at the far end of the pond at mid-depth.
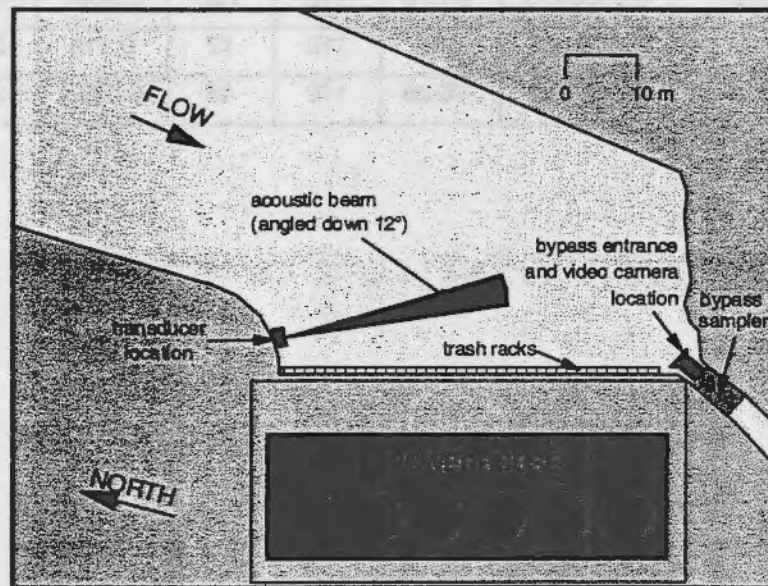
Figure 2. Plan view of Cabot Station forebay showing position of transducer, orientation of acoustic beam, and bypass. Forebay depth is approximately 10 m.

Fig. 2
Figure 3. Observed target strengths (dB) of a 685 mm a) dorsally and b) laterally oriented American eel plotted as a function of pulse number.

Fig. 3
Figure 4. Observed target strengths (dB) of a 685 mm a) dorsally and b) laterally oriented American eel plotted as a function of range (m) from transducer.
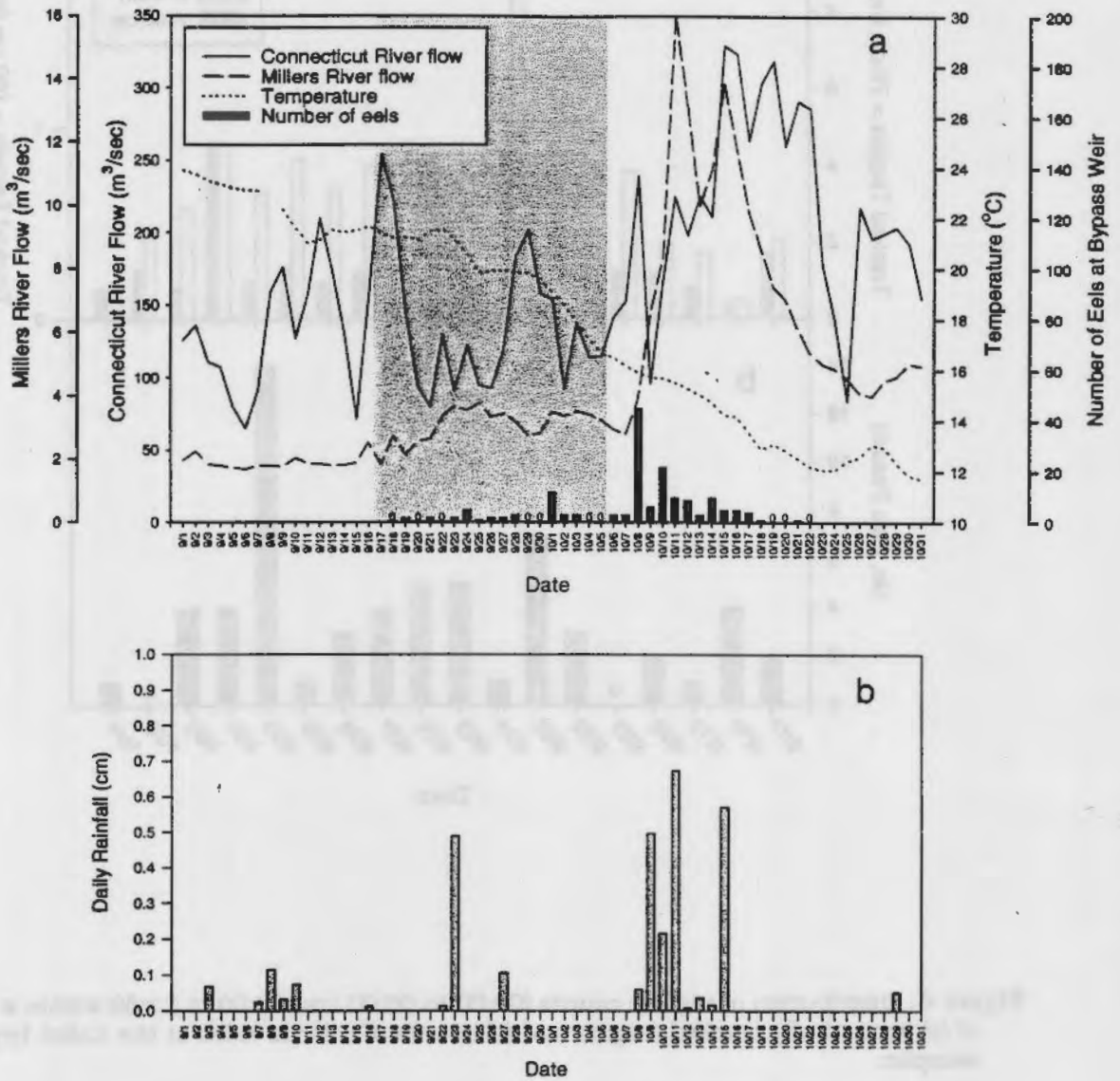
Figure 5. (a) Flow and temperature data from the Connecticut and Millers Rivers, September –
October, 1998, and video counts of eels at the Cabot bypass weir during the evening hours
(17:00 – 22:00): gray zone indicates period of hydroacoustic monitoring, and videotapes were
analyzed only for the period from 18 September to 22 October. (b) Daily rainfall data from
Sunderland, Massachusetts.
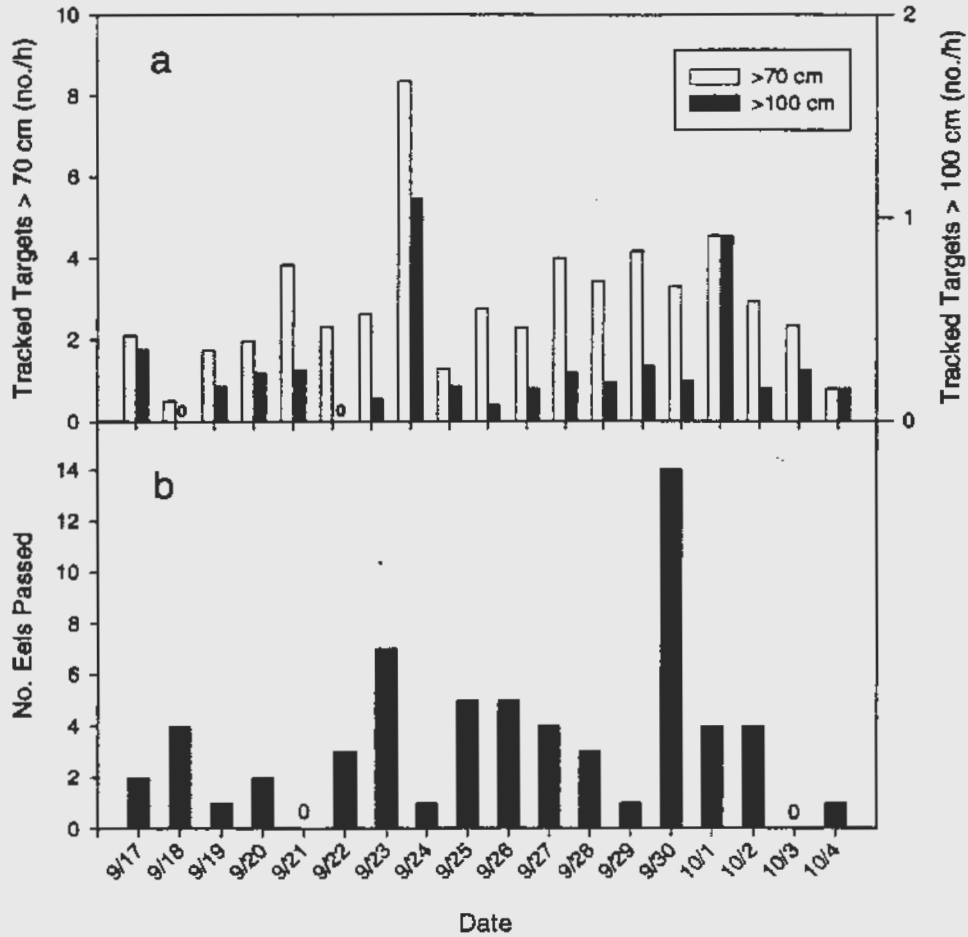
Figure 6. Distribution of nightly counts (00:00 to 06:00 and 18:00 to 23:59 within a single date) of (a) acoustically tracked targets and (b) counts of eels via video at the Cabot bypass sampler.
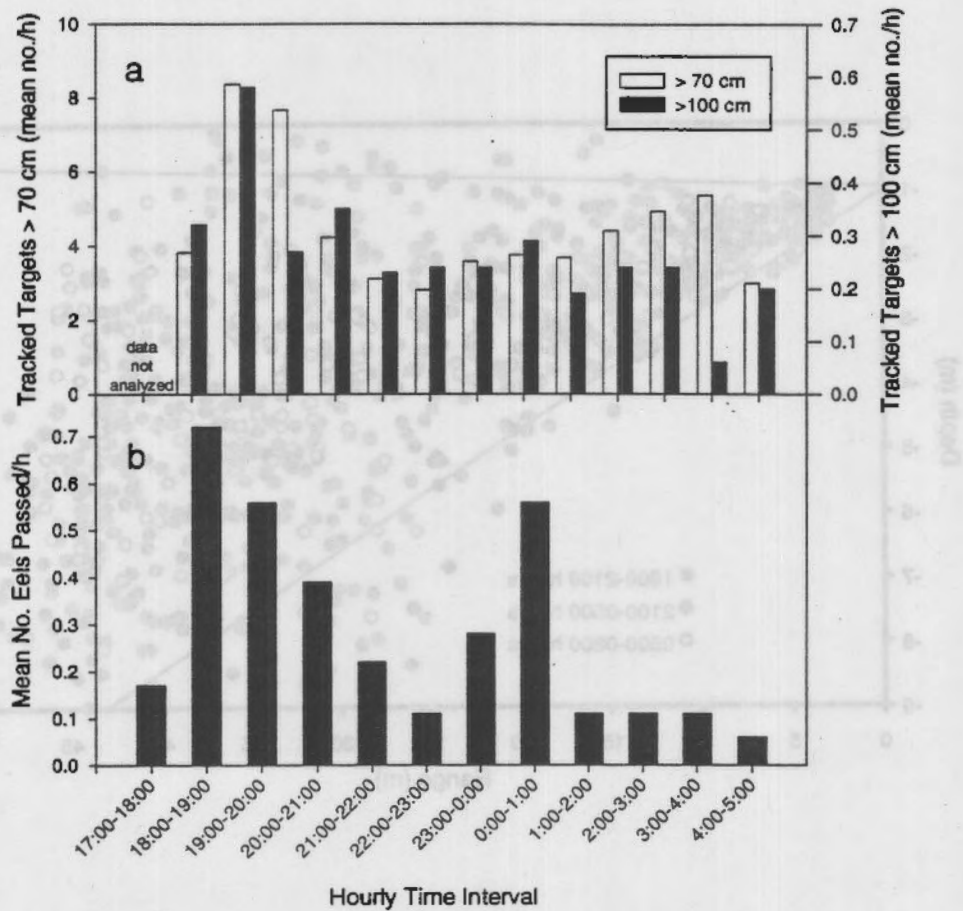
Figure 7. Diel distribution of (a) mean number of acoustically tracked targets and (b) video counts of eels the Cabot bypass sampler from 17 September to 4 October. Acoustic data from 17:00 to 18:00 were not analyzed due to incomplete sampling (no data from 6 of 18 days) during this time interval.
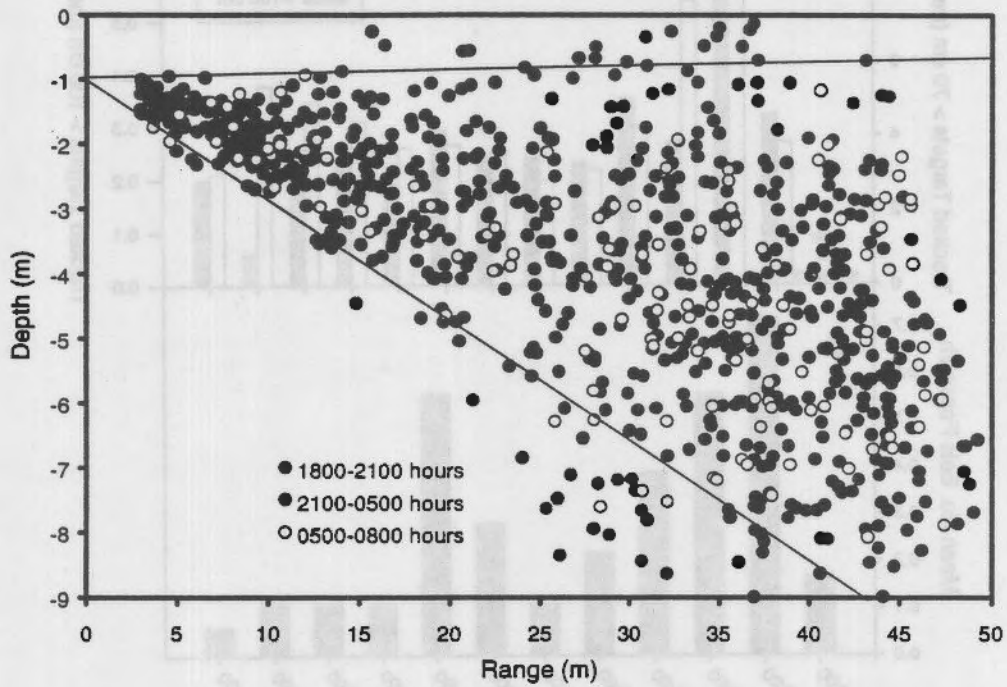
Figure 8. Range and depth distribution of tracked fish > 70 cm grouped by 3 hour intervals. The sample area for the transducer beam is depicted with the solid lines extending from the transducer (mounted at range 0 and depth of 1 m).

25
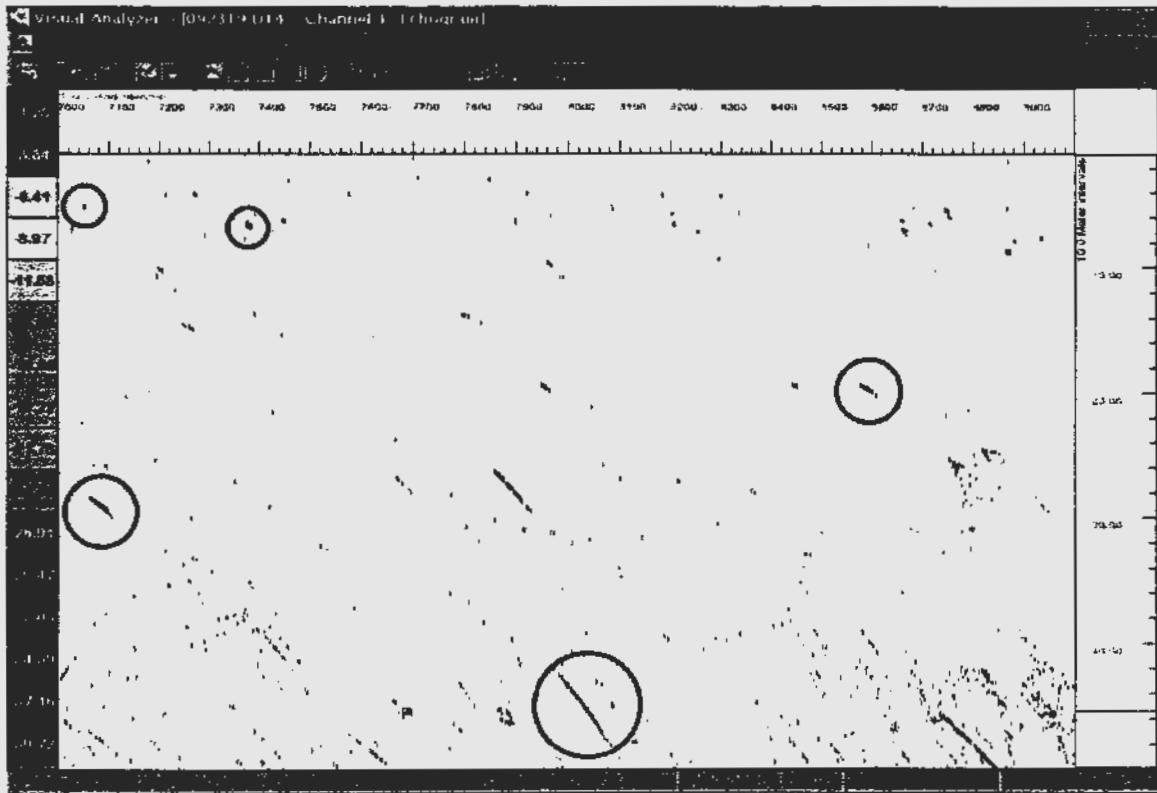
Figure 9. Echogram of tracked fish September 23 1923 - 1930 hours with 5 tracked fish (circles) exceeding a target strength of –28.8 dB (100 cm).
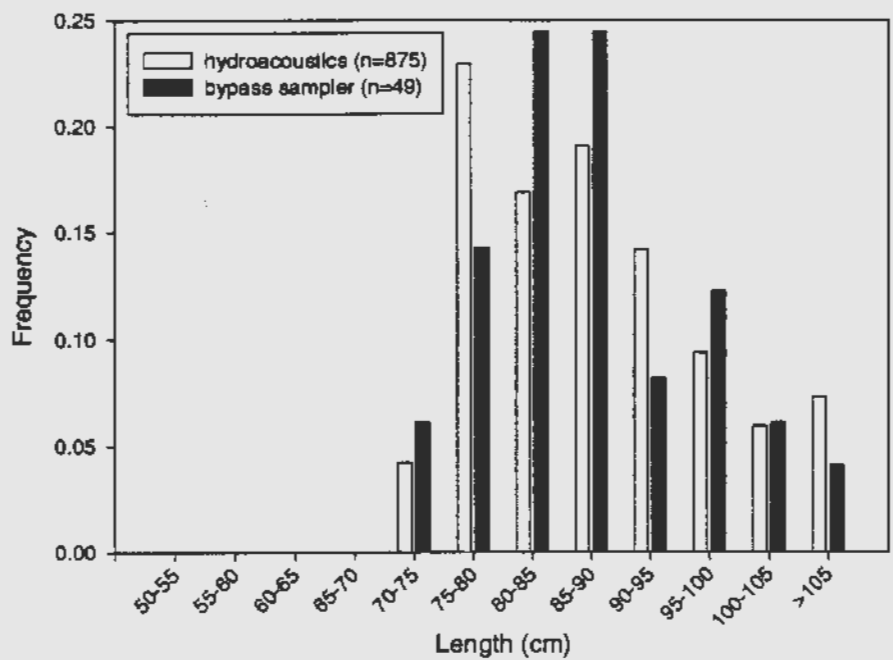
Figure 10. Distribution of lengths of eels captured at the Cabot Station bypass sampler in 1996 and 1997 and estimated by 1998 hydroacoustic target strength. Hydroacoustic data only includes targets >70 cm.

a. dorsal
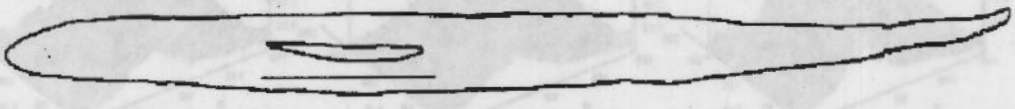
b. lateral

10 cm

Fig. 1

Figure 11. Schematic diagrams of a) dorsal and b) lateral orientations of a 660 mm American eel (*Anguilla rostrata*) body and swimbladder. Silhouettes are traced from radiographs, scanned, and then digitized at 1 mm resolution.

28

a b c

d e

modeled length 540 mm
theta range 70˚-110˚
frequency range 12-420 kHz
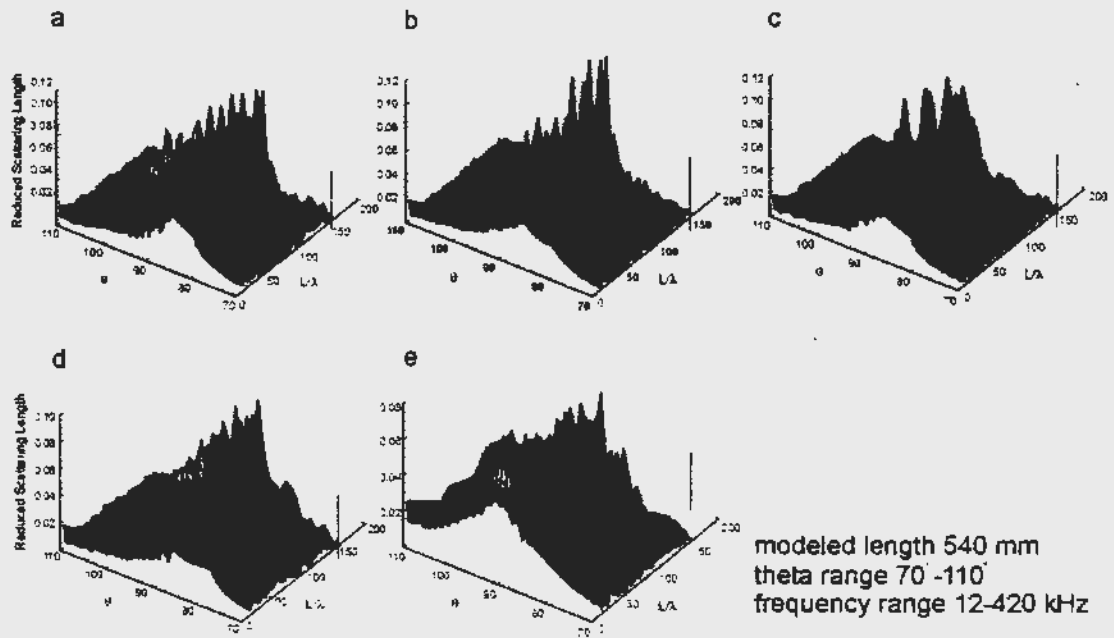
Fig. 4
Figure 12. Kirchhoff-ray mode predicted dorsal, reduced scattering lengths of five American eels (*Anguilla rostrata*) as a function of fish aspect θ, length L, and acoustic wavelength λ. All eels were modeled at a length of 540 mm, an aspect range of 70° to 110°, and a frequency range of 12 kHz to 420 kHz. Original eel lengths were: a) 608 mm, b) 660 mm, c) 691 mm, d) 366 mm, and e) 372 mm.

modeled length 540 mm
theta range 70°-110°
frequency range 12-420 kHz
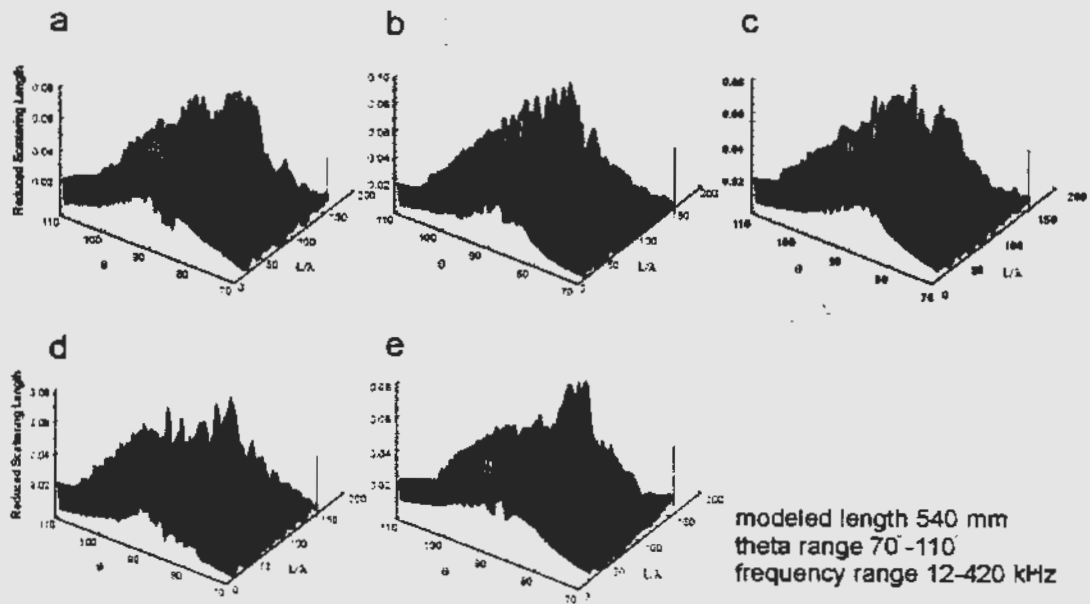
Fig. 5
Figure 13. Kirchhoff-ray mode predicted lateral, reduced scattering lengths of five American eels
(*Anguilla rostrata*) as a function of fish aspect θ, length L, and acoustic wavelength λ. All eels
were modeled at a length of 540 mm, an aspect range of 70° to 110°, and a frequency range
of 12 kHz to 420 kHz. Original eel lengths were: a) 608 mm, b) 660 mm, c) 691 mm, d) 366
mm, and e) 372 mm.
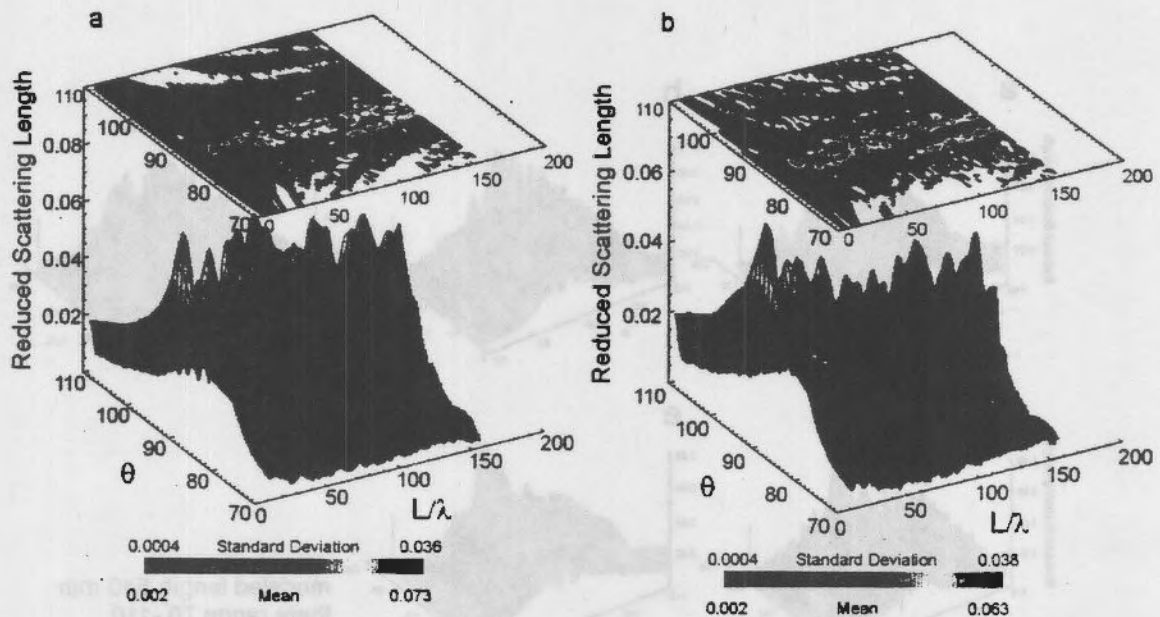
Fig. 6

Figure 14. Kirchhoff-ray mode predicted mean and standard deviation reduced scattering
lengths of five American eels (*Anguilla rostrata*) from a) dorsal and b) lateral perspectives.
Reduced scattering lengths are plotted as a function of fish aspect θ, length L, and acoustic
wavelength λ. All eels were modeled at a length of 540 mm, an aspect range of 70° to 110°,
and a frequency range of 12 kHz to 420 kHz.

Fig. 7
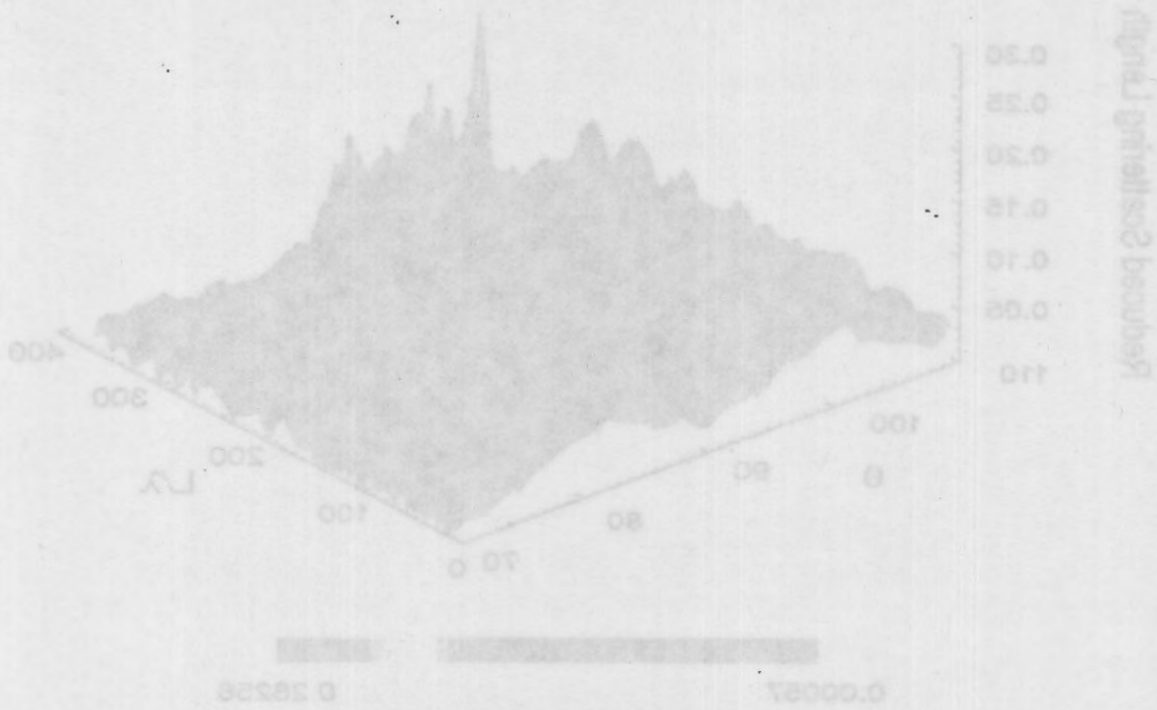
Figure 15. Kirchhoff-ray mode 420 kHz predicted a) dorsal and b) lateral mean and standard deviation target strengths of five American eels (*Anguilla rostrata*) (from Figs. 4 and 5) plotted as a function of fish length. Observed dorsal and lateral mean and standard deviation target strengths are overlayed for six eels used in target strength measures.
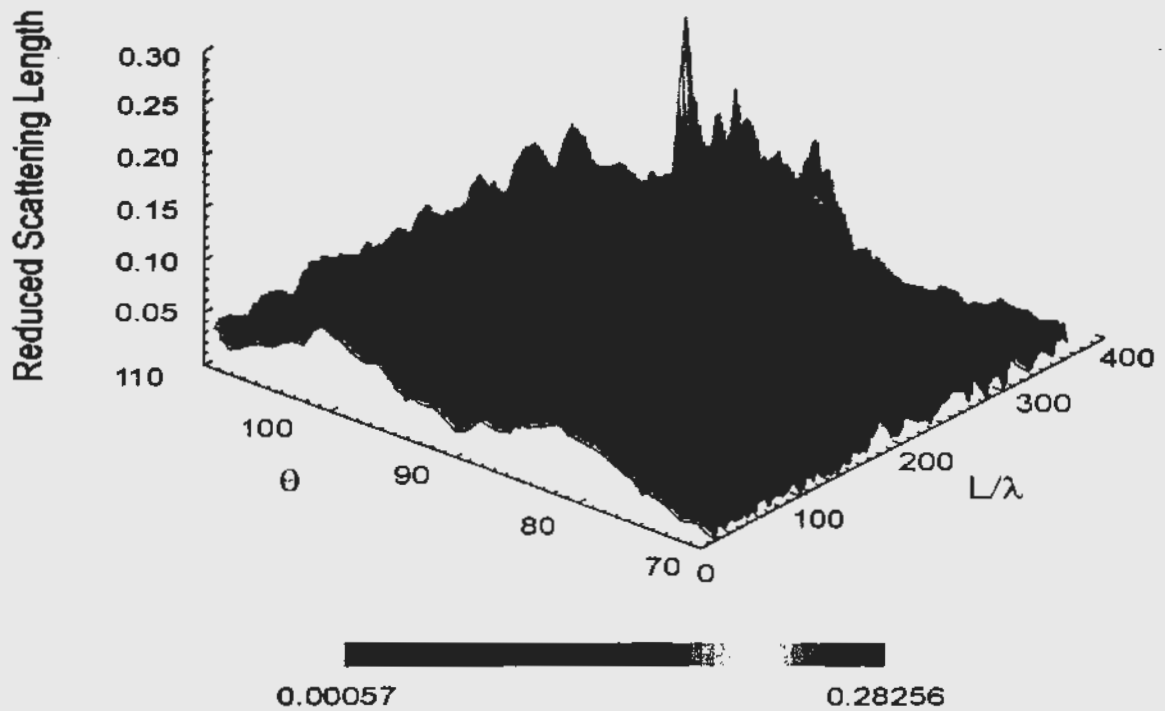
Fig. 8

Figure 16. Kirchhoff-ray mode predicted dorsal, reduced scattering lengths of a New Zealand
   longfinned eel (*Anguilla deiffenbachii*) as a function of fish aspect θ, length L, and acoustic
   wavelength λ. The eel was modeled at a length of 1260 mm, an aspect range of 70° to 110°,
   and a frequency range of 12 kHz to 420 kHz.
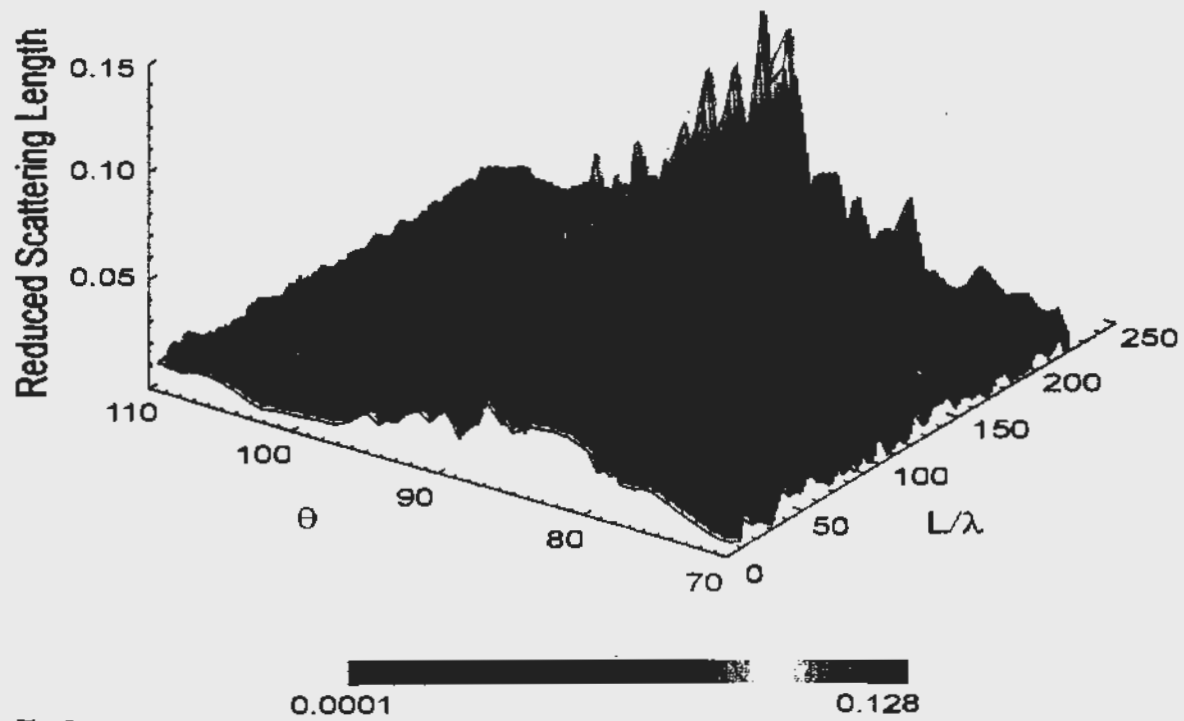
Fig. 9

Figure 17. Kirchhoff-ray mode predicted dorsal, reduced scattering lengths of a New Zealand shortfinned eel (*Anguilla australis*) as a function of fish aspect θ, length L, and acoustic wavelength λ. The eel was modeled at a length of 765 mm, an aspect range of 70° to 110°, and a frequency range of 12 kHz to 420 kHz.